Waste and Biomass Valorization (2021) 12:4419–4431
https://doi.org/10.1007/s12649-020-01334-5

ORIGINAL PAPER

Application of Photocatalysis Methods to Enhance Sludge Disintegration

Sayiter Yildiz[1] · Asaad Olabi[1]

Received: 29 August 2020 / Accepted: 18 December 2020 / Published online: 4 January 2021

Abstract

This paper investigated the disintegration of waste sludge with different photocatalytic processes. For this objective, the effects of initial pH, reaction time, TiO_2 amount with Fe^{2+}, Fe^0 and H_2O_2 doses on the disintegration degree (DD) were determined. Soluble chemical oxygen demand (SCOD) was used as the main parameter in the study. Process optimizations, kinetic study and Disintegration degree calculation were performed based on the SCOD parameter. In order to observe the effect of UV light, UV-A, UV-B, UV-C lights were used, and the best DD was determined. In addition, SEM analyzes were performed to determine Particle Size Distribution, toxicity and sludge characterization in raw sludge and disintegrated sludge. As a result of optimization studies, optimum pH 3, reaction time 60 min, 6 g/kg TS Fe^{2+}, 4 g/kg TS Fe^0, 40 g/kg TS/20 g/kg TS H_2O_2 and 0.8 g/l TiO_2 doses were obtained. The highest DD was obtained in the $TiO_2/Fe^0/H_2O_2$/UVB process with 69.49%, while the lowest DD value was obtained in the TiO_2/Fe^{2+}/UVC and TiO_2/Fe^0/UVC processes with 15.25%. Results suggest that the amount of sludge was reduced between 19.2% and 34.6% by photocatalytic disintegration. As a result, it was concluded that the Photocatalysis process is a feasible and efficient process for disintegration of sludge.

✉ Sayiter Yildiz
sayiteryildiz@gmail.com

[1] Engineering Faculty, Department of Environmental Engineering, Cumhuriyet University, 58140 Sivas, Turkey

Graphic Abstract

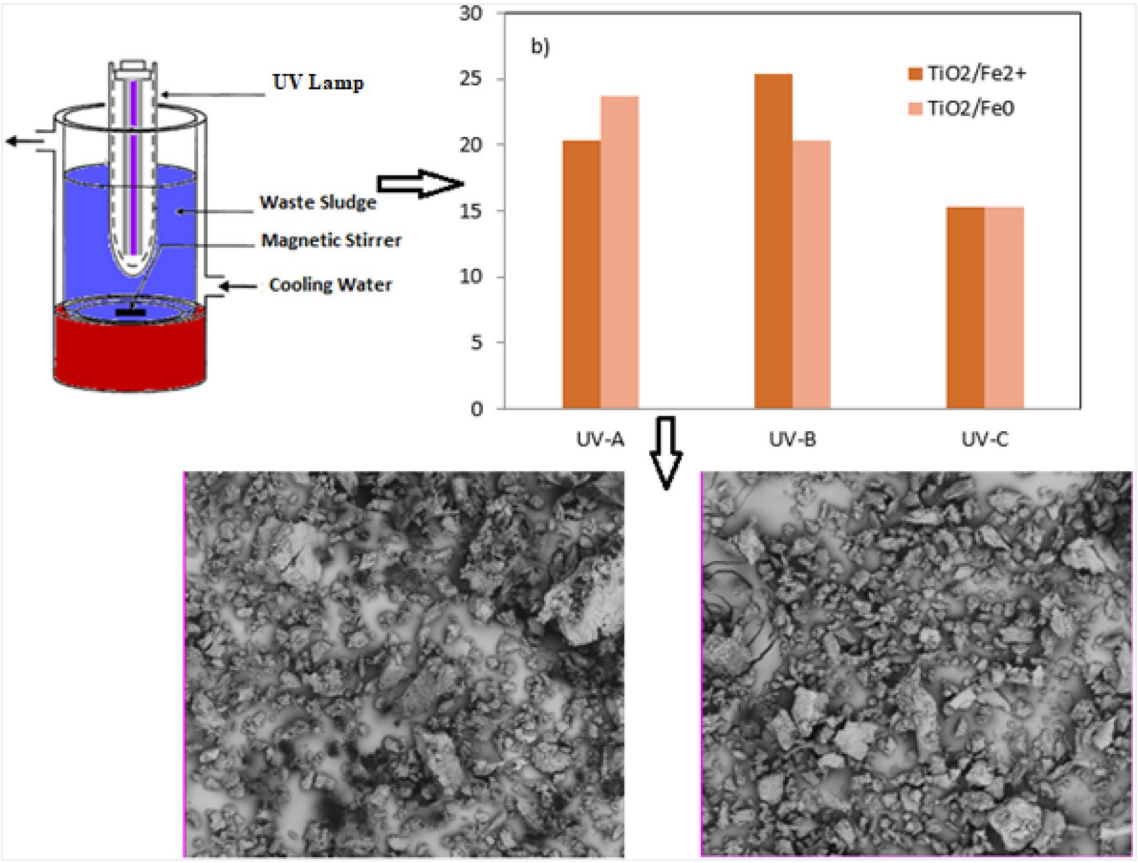

Keywords Sludge disintegration · Photocatalysis · TiO_2 · UV · H_2O_2

Statement of Novelty

This work contributed to the disintegration of waste sludge with different photocatalytic processes. Considering the initial pH, reaction time, TiO_2, amount with Fe^{2+}, Fe^0 and H_2O_2 doses and different UV, a holistic approach was proposed for the disintegration of waste sludge. In order to observe the effect of UV light, different wavelengths; UV-A (365 nm), UV-B (302 nm), UV-C (256 nm) were applied and the most suitable wavelength was determined. In addition to the toxicity analysis, Particle Size Distribution, SEM analyzes were also performed to determine sludge characterization.

Introduction

In recent years, attention has been paid to minimize the amount of sludge in the waste water treatment process. The treatment and disposal of waste sludge is about half the entire operating cost for municipal wastewater treatment plants. Therefore, researches on sludge treatment are increasing and some new sludge reduction techniques are recommended [1–3]. One of the sludge reduction techniques is sludge disintegration.

Sludge disintegration can be accomplished by degradation of sludge flora or microorganism cells in the sludge depending on the type and the intensity of disintegration [4]. By means of disintegration, the degree of sludge stabilization increases. In addition, less sludge production and more biogas production are provided [5]. In recent years, sludge disintegration has been carried out with some processes; Fenton [6], electrocoagulation [7], ultrasound energy [8], high pressure [9], thermal energy [10], enzymes [11], Hydrocyclone pretreatment [12], Ultrasonic disintegration [13]. Different chemical techniques are often applied for WAS disintegration [14]. Current results reveal the great potential of chemical technology in reducing excess sludge production [1]. The application of AOP often leads to the by-products formation and to an increase the toxicity of the

treated water [15]. The Photo-Fenton reaction, one of the advanced oxidation processes (AOP), can offer a promising technology to minimize excess sludge [16].

AOP includes heterogeneous photocatalysis processes using semiconductors such as TiO_2 and ZnO, and homogeneous processes such as Fenton process, H_2O_2 and ozone. Among these processes, Fenton process and TiO_2 attract more attention, especially when applied with ultraviolet (UV) radiation [17, 18]. Up to 80% of catalytic processes are involved in heterogeneous catalysis, making this process a vibrant branch of chemistry [19].

TiO_2 is a semiconductor with high photocatalytic activity, is relatively inexpensive and has good stability in the aqueous solution [20]. The advantages of using a degradation process using photocatalytic phenomena have been indicated in several studies. These advantages include: fast reaction, less sludge production, high repeatability and relatively low cost [21, 22].

The photocatalytic properties of TiO_2 are derived from the formation of photogenerated charge carriers (gaps and electrons) that occur upon absorption of ultraviolet (UV) light corresponding to the band gap [23, 24]. TiO_2 surfaces become superhydrophilic with less than 5° contact angle under UV light irradiation [25]. Superhydrophilicity results from changes in the chemical structure of a surface. If the semiconductor is exposed to a certain wavelength of light, electrons are excited to move from the valence band to the conduction band and a gap is created in the valence band [26]. This process takes place in the early stages of a photocatalyst reaction.

TiO_2 has a high light absorption ability, characterized by the band gap energy (Eg) value corresponding to 3.2 eV for the anatase structure. When light with the hv energy equal to or greater than the bandgap energy (Eg) is used, the electrons in the valence band have enough energy to be able to move or be excited to the conduction band and leave the positive hole (hv +) in the valence band (Eq. 1) [27]:

$$TiO_2 + hv \rightarrow e^-_{cb} + hv^+_{vb} \quad (1)$$

Gaps in the valence band can act with H_2O to produce hydroxyl radicals and other reactive oxygen species (Eq. 2):

$$hv^+_{vb} + H_2O \rightarrow OH\bullet + H^+ \quad (2)$$

This reaction is a kind of advanced oxidation technique and is the beginning of the next photocatalytic reaction [26]. If other oxidizing agents such as hydrogen peroxide or ozone are available, additional hydroxyl radicals can be generated under UV irradiation. Irradiation of hydrogen peroxide with UV light produces OH• known to react with a large number of chemicals, but the formed radicals are unstable. The formation of OH• by photolysis of H_2O_2 with UV light is given in Eq. 3 below.

$$H_2O_2 + hv \rightarrow 2OH\bullet \quad (3)$$

UV/Oxidation Technologies take place either in a homogeneous environment with addition of a suitable oxidant substance (hydrogen peroxide or ozone) or in a heterogeneous environment containing semiconductor particles (eg titanium dioxide) [28]. In the Fenton process, OH• is produced by reacting hydrogen peroxide with Fe^{2+} and Fe^{3+} salts [29].

Yu et al. [30] have examined the treatability of H-acid (1-amino-8-naphthol-3, 6-disulphonic acid) by photocatalytic oxidation method (TiO_2/UVA). Noorjahan et al. [31] have investigated the heterogeneous photocatalytic degradability of H-acid that is toxic and non-biodegradable. Mohanty et al. [32] have used the TiO_2/UV-A combined photocatalytic process to achieve an improved biodegradability of H-acid. Sauer et al. [33] have tried to treat leather wastewater with AOP (H_2O_2/UV, TiO_2/H_2O_2/UV and TiO_2/UV). Arana et al. [34] have studied the photocatalytic degradation of organic substance by applying UV/TiO_2 method to wastewater in the presence of some ions such as ozone and some phosphate. Muruganandham et al. [35] have used three different AOPs (UV/H_2O_2/Fe^{2+}, UV/TiO_2 and UV/H_2O_2) in removal of reactive azo dyestuff. Catalkaya and Kargi [36] have investigated the TOC and toxicity removal in pulp wastewater by UV, UV/H_2O_2, UV/TiO_2, UV/H_2O_2/TiO_2 methods. Garcia et al. [37] have studied pollution removal in textile wastewater by UV/H_2O_2, UV/TiO_2, UV/TiO_2/H_2O_2 and UV/Fe^{2+}/H_2O_2 methods.

UV/Fenton/TiO_2 application has been reported extensively in the literature, but there is a published literature shortage on sludge disintegration. In this study, the disintegration of the sludge taken from the wastewater treatment plant was investigated with different Photo catalytic processes. In this context, effects of of initial pH, reaction time, TiO_2, iron and H_2O_2 doses under different UV light were determined. Soluble Chemical Oxygen Demand (SCOD) was selected as the target parameter. Process optimizations, kinetic study and DD calculation were performed based on SCOD parameter. In order to observe the effect of UV light, different wavelengths; UV-A (365 nm), UV-B (302 nm), UV-C (256 nm) were applied and the most suitable wavelength was determined. In addition to the toxicity analysis, Particle Size Distribution, SEM analyzes were also performed to determine sludge characterization.

Experiments were performed in triplicate and the average values of samples were presented. Data presented are the mean values from the experiments, standard deviation ($\leq$4%) and error bars are indicated in figures.

Materials and Methods

Many of suspended solids in the activated sludge are of organic substance. Since most active sludge microorganisms will be killed and oxidized to organic substances, the effects

of sludge reduction can be determined in terms of changes in SCOD [38, 39]. In this study, separate experiments were carried out to determine the effect of parameters such as TiO_2, Fe^{2+}/Fe^0 and H_2O_2 concentrations, pH, contact time and UV light at different wavelengths on the DD and the amount of SCOD. The three different UV light sources used are UV-A (365 nm), UV-B (302 nm), UV-C (256 nm). In addition, in order to observe the effect of photocatalytic disintegration on particle degradation of the sludge, SEM and toxicity analyzes were performed.

Waste Activated Sludge (WAS)

The WAS sample used in the experimental studies was supplied from the return line of Sivas domestic wastewater treatment plant in Turkey. Samples were stored in refrigerator at + 4 °C. The WAS has features such as pH 6.5, SCOD 48 mg/L, total COD 9800 mg/L, total solids (TS) 8285 mg/L, suspended solid (SS) 5950 mg/L, electrical conductivity (EC) 1040 µS/cm, and a TS content of 1%.

Synthesis of Zero-Valent Iron Nanoparticle (Fe^0)

5.34 g $FeCl_2 \cdot 4H_2O$ was mixed in a 30 ml solution (24 ml ethanol + 6 ml distilled water) in a magnetic stirrer. Elsewhere, 1 M $NaBH_4$ (3.05 g $NaBH_4$ in 100 mL distilled water) was prepared. The prepared $NaBH_4$ solution was added dropwise to the Fe solution mixed in the magnetic stirrer. As soon as $NaBH_4$ was added, black mud has begun to form. After adding $NaBH_4$ completely, mixing was continued in the mixer for another 10 min. The black mud formed was separated by centrifuge. It was centrifuged repeatedly by washing with 25 mL ethanol. It was dried at 500 °C until it was completely dry. It was kept in a desiccator in order to prevent the material from getting moisture and stored in a closed box [40].

Optimization Studies

Iron Dose Optimization

Oxidation was performed by applying different amounts of iron to each reactor, keeping other parameters (pH = 3, time = 60 min, H_2O_2 = 40 g/kg TS) constant. After the sample was passed through 0.45 micron filter paper, SCOD analyzes were performed and DD was calculated. An optimum dose was determined by evaluating the results obtained for each iron dose.

H_2O_2 Dose Optimization

By keeping the optimum iron dose -determined in the previous stage- and other parameters (pH = 3, time = 60 min), different amounts of H_2O_2 were dosed in each reactor and optimum H_2O_2 dose was determined by following the same procedure.

pH Optimization

The optimum iron and H_2O_2 dose determined in the previous stage was kept constant and applied to each reactor for 60 min at different pHs, thus oxidation was carried out and the optimum pH was determined by following the same process sequence.

TiO_2 Optimization

Oxidation was achieved by applying different amounts of TiO_2 using pH 3, time 60 min and UVA light. SCOD analysis was done and DD was calculated in samples. The optimum dose was determined by evaluating the results obtained for each TiO_2 amount.

Reaction Time

In this study, oxidation was performed at different times (0–150 min) by keeping pH 3 and optimum TiO_2 dose constant. The optimum time was determined according to the results obtained.

Fenton Oxidation

The experiments with Fe^{2+} were carried out using stock solution of H_2O_2 and $FeSO_4.7H_2O$ salt as fenton reagent. 0.1 and 1 N H_2SO_4 solutions were used to adjust the initial pH of raw sludge to acidic conditions. After adjusting pH to desired value, the doses of Fe^{2+} ($FeSO_4.7H_2O$) and H_2O_2 (35% H_2O_2 solution) were added respectively. After dosing the hydrogen peroxide, 1 h reaction time was considered to have started. Experiments were carried out in 250 ml glass beakers for raw sludge sample in 250 ml liquid volume. The same method was used in Fe^0 experiments. But, instead of ferro iron, metallic iron powder (Fe^0) was used.

Photo-Fenton Oxidation

In order to determine the effect of UV on the sludge disintegration process, experiments were carried out with UV-A, UV-B, UV-C light. The optimum amounts of iron, H_2O_2 and TiO_2 obtained as a result of optimization were used in the experiments. The reactor in which the study was carried out is shown in Fig. 1.

Analysis

The COD and SCOD were done according to procedures given in Standard Methods [41]. The pH and EC of the

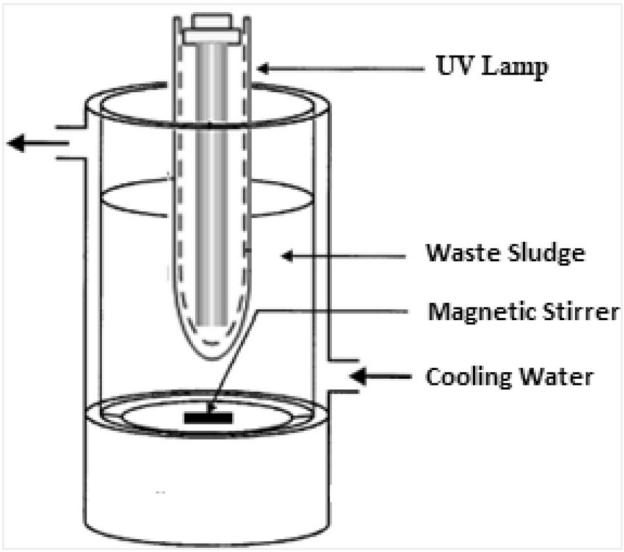

Fig. 1 Photocatalytic oxidation application reactor

sludge were measured by using a pH meter (Thermo Orion – STARA2145). Particle Size Distribution analyses were conducted with a Malvern Mastersizer 2000QM brand particle size analyzer.

Disintegration Degree (DD)

To assess the sludge disintegration performance, the degree of disintegration (DD) was calculated using Eq. 4 [42].

$$DD(\%) = \frac{SCOD_S - SCOD_{SO}}{SCOD_{NaOH} - SCOD_{SO}} \times 100 \quad (4)$$

here, $SCOD_S$ Soluble COD value of disintegrated sludge (mg/L), $SCOD_{SO}$ Soluble COD value of non-disintegrated sludge (raw sludge) (mg/L), $SCOD_{NaOH}$ Soluble COD value of chemically disintegrated sludge at room temperature, 20 ± 1 °C, 24 h with 1 mol/L NaOH (mg/L).

Toxicity

Seed Germination Test expressing toxicity was performed for raw and disintegrated sludge with different applications. The emergence of radicals in the Petri dish indicates seed germination [43]. Sludge samples were filtered by vacuum filtration. Afterwards 10 mL of filtrate was transferred to Petri dish and ten spinach seeds (Spinacia oleracea) were placed in each petri dish. It was incubated at 28 °C. The test was carried out for 10 days. Seeds (germinated) from which their radicals began to appear were counted. The germination percentage (GP) was calculated using Eq. 5 below [44]:

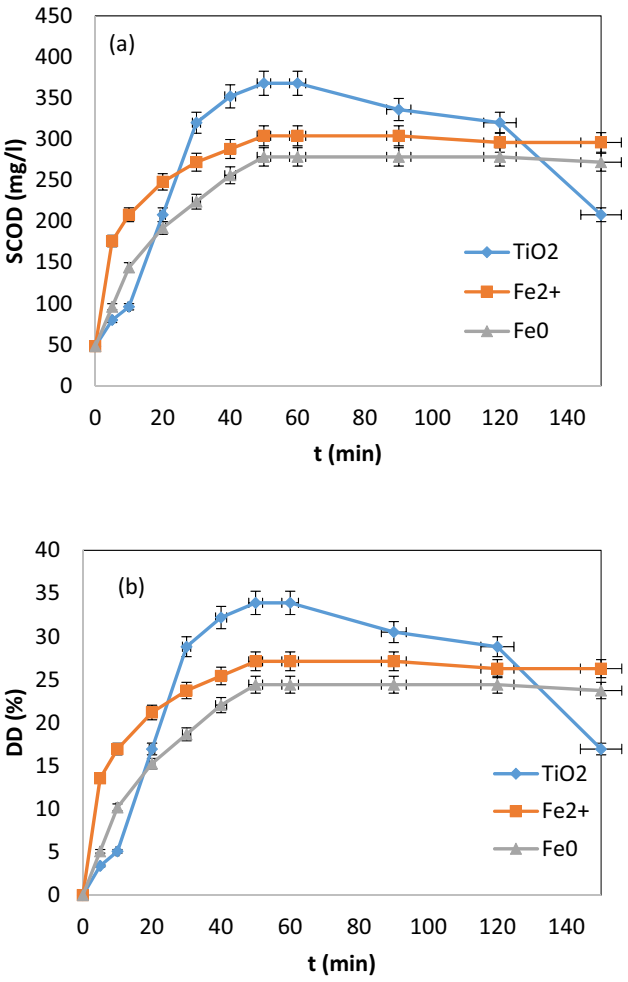

Fig. 2 SCOD (**a**) and DD (**b**) Changes depending on the reaction time

$$GP = \frac{\text{Number of seeds germinated}}{\text{Number of seeds planted}} \times 100 \quad (5)$$

Results and Discussion

Determination of Reaction Time

TiO_2/UV, Fe^{2+}/H_2O_2/UV and Fe^0/H_2O_2/UV processes were applied in this study. To determine the reaction time of each process, TiO_2 0.8 g/L; Fe^{2+} 6 g/kg TS, H_2O_2 40 g/kg TS; Fe^0 4 g/kg TS, H_2O_2 20 g/kg TS, UVA and pH 3 were kept constant. In these conditions, the change of SCOD and DD depending on time was examined at room temperature, and the results are given in Fig. 2. The reaction time being long or short is an indicator of the degradability of organic substances in the structure of sludge. The short time required for degradation shows that there are organic substances which deteriorate easily in the structure of sludge, while the long

time references the presence of hardly deteriorate organic substances [45].

As seen in Fig. 2, in the first 10 min the oxidation reaction occurred rapidly in Fe^{2+} usage since there was sufficient amount of catalyst ferro iron and H_2O_2, while it took place more slowly in Fe^0 usage because it depends on the dissolution of metallic iron. A similar status is acceptable for the use of TiO_2. In all three processes, the speed of the rise of SCOD slows down as a result of the decrease of reaction components in the environment over time. It is seen that the disintegration of the sludge is carried out in two phases. In Fe^{2+} usage, it was determined that the fast oxidation phase in the first 5 min and the remaining 55 min were the slow oxidation phase. In Fe^0 usage, it was observed that the reaction took place later due to the dissolution of iron, and rapid oxidation in the first 10 min, while the reaction slowed down in the next 40 min.

In the reaction with TiO_2, it can be seen that the chemical oxidation is roughly divided into two phases. After adding TiO_2 to the solution in the photoreactor, the SCOD increased and reached a maximum after about 60 min (phase I). At this phase, some activated sludge microorganisms were killed and oxidized to organic substances dissolved by photocatalytic reaction. As a result of the oxidation, organic substances were leached into the supernatant and the SCOD increased [46, 47]. Later, there was a decrease in SCOD (phase II). Mineralization of dissolved organic substances by photocatalytic reaction may be dominant in phase II [46]. In phase I, in the beginning, the amount of COD solubilized by the photocataliysis reaction was superior to that of dissolved organic substances mineralized by the photocataliysis reaction. On the other hand, the solubilization rate in phase II is slower than the mineralization rate. This change in SCOD shows similarity to those in Déléris et al. [48], Egemen et al. [46], Vlyssides and Karlis [49] studies. In this study, the optimum time was determined as 60 min for all three processes.

Effect of Catalyst (Fe^{2+}, Fe^0) Concentration

A specific or average iron concentration is not recommended for Fenton process studies. Because both the wastewater characteristics and the ambient temperature at which the reaction takes place are important factors in determining the concentration of Fe^{2+} to be applied [50]. The optimization of Fe^{2+} and Fe^0 was studied at a time of 60 min, pH 3 at 40 g/kg TS H_2O_2 concentration and in the range of 2, 4, 6, 10, 30 g/kg TS iron concentration. DD changes depending on the iron dose are given in Fig. 3.

As will be seen in the fenton reaction given in Eq. 6, Fe^{2+} ion reacts with H_2O_2 to form OH•. When the concentration of Fe^{2+} ion increases according to the reaction, the resulting OH• will increase, and accordingly the AOP

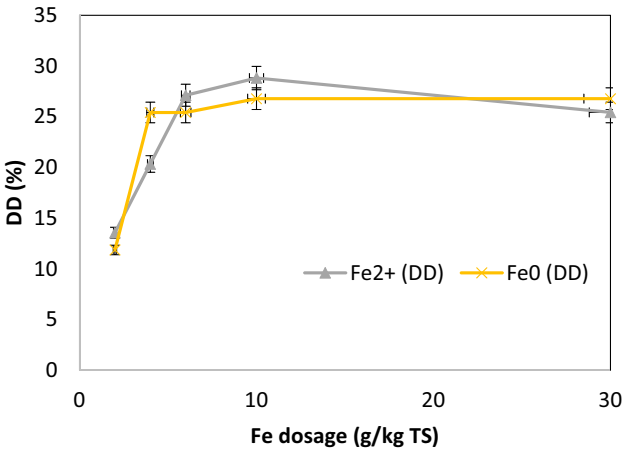

Fig. 3 DD changes depending on Fe^{2+} and Fe^0 Dose (2–30 g/kg TS)

performance will improve [51]. However, the positive effect of this increase in Fe^{2+} ion concentration is not linear. Fe^{2+} ion concentration above a certain level decreases the reaction rate. At the same time, excess Fe^{2+} in the medium may increase the amount of SS, leading to excessive sludge formation at the process exit [52].

$$Fe^{2+} + H_2O_2 \rightarrow Fe^{3+} + OH\bullet + OH^- \quad (6)$$

It is seen in Fig. 3 that the rate of degradation of organic substance increases in parallel with the increase of Fe^{2+} ion concentration in the reaction medium. However, the increase continued until a certain concentration. Above this concentration, it was found that the rate of disintegration of organic substances in the Fenton process decreases. This event has been observed in similar studies [53–55].

As seen in Fig. 3, the maximum DD 28.81% at 10 g/kg TS Fe^{2+} concentration was obtained when using Fe^{2+}. In Fe^0, with the increase in the applied Fe^0 dose, up to 10 g/kg TS Fe^0 concentration, there was a steady increase in DD. This increase was remarkable up to 4 g/kg TS Fe^0 dose, but at negligible levels at higher doses. The radical scavenging effect of excess iron in Fe^{2+} process was not observed in Fe^0 process, since metallic iron powder takes time to dissolve in the sludge and ferro iron is not given suddenly, as in Fe^{2+} process. As a result, considering the economic conditions, while the dose of 6 g/kg TS Fe^{2+}, where 27.12% DD has been provided, was determined as optimum dose in Fe^{2+} process; The dose of 4 g/kg TS Fe^0, where 25.42% DD has been obtained, was determined as optimum dose in Fe^0 process.

Effect of H_2O_2 Dose

In Fenton process, process performance improves when the amount of H_2O_2 is increased up to a certain value, similar

to Fe^{2+} ion. Because H_2O_2 is the source of OH• radicals formed by the fenton reaction. Increasing the amount of H_2O_2 and getting away from its optimum level increases the process cost, and excess H_2O_2 reacts with OH•, leading to formation of HO_2• (Eq. 7), which has much lower oxidation power [52].

$$H_2O_2 + OH\bullet \rightarrow H_2O + HO_2\bullet \quad (7)$$

In H_2O_2 optimization study, duration of 60 min, pH 3, 6 g/kg TS for Fe^{2+} and 4 g/kg TS for Fe^0 and 5, 20, 40, 50 g/kg TS H_2O_2 concentrations were applied. The results are shown in Fig. 4.

Determination and application of effective H_2O_2 concentration in Fenton process is very important in terms of treatment efficiency. Because a certain increase in the amount of H_2O_2 increases COD and color removal. However, at higher concentrations excessive H_2O_2 remaining in the medium without reacting causes COD interference [56].

As seen in Fig. 4, DD continuously increased up to 40 g/kg TS H_2O_2 concentration in Fe^{2+} process. Between 40 and 50 g/kg TS H_2O_2 concentration, DD remained constant. Whereas, in Fe^0 process, up to 20 g/kg TS H_2O_2 dose, DD increased significantly, there was a slight increase with increasing dose to 40 g/kg TS. At higher dose, an increase in DD was not detected. Thus, optimum H_2O_2 concentrations were determined as 40 g/kg TS H_2O_2 for Fe^{2+} and 20 g/kg for Fe^0. The results obtained in the study are similar to those in previous studies [57, 58].

Photo Fenton Process

The process performed by applying UV light and fenton reactions in the same reactor is called photo-fenton process [59–61]. Equation 8 shows the photo-fenton reaction mechanism. Fe^{3+} ions formed during the Fenton reaction are reduced to Fe^{2+} ions by UV effect, but the concentration of Fe^{2+} ions formed is lower than the initial Fe^{2+} concentration. Fe^{2+}, which is formed as a result of the photo-fenton reaction, enters the fenton reaction again. Reactions 6 and 8, which enter into a cycle in this way, also increase the effectiveness of the fenton process due to the OH• they form at each step [62, 63].

$$Fe^{3+} + H_2O_2 + h\nu \rightarrow Fe^{2+} + OH^- + OH\bullet \quad (8)$$

Effect of TiO_2 Dose

TiO_2 widely studied and used in many applications due to its strong oxidizing abilities [64], super hydrophilicity [25], chemical stability, long durableness, toxicity and low cost. In this study, the initial conditions were determined as pH 3, UVA lamp and duration 60 min to determine the effect of consentration of TiO_2. TiO_2 consentration was changed between 0.05 and 1 g/l (Fig. 5), and the optimum TiO_2 dosage for disintegration with photocatalyst was determined.

As seen in Fig. 5, DD amount started to increase with increasing TiO_2 consentration, and this increase continued until the use of 0.8 g/l TiO_2. After that value, DD started to decrease. For this reason, the optimum consentration of TiO_2 was determined as 0.8 g/l.

Effect of pH

The pH values of solutions directly or indirectly affect the oxidation of organic substances [65]. The pH of solution controls the speed of hydroxyl radical production. Therefore, pH is an important parameter for the PhotoFenton-Photocatalytic process. In order to determine the pH effect on photocatalytic disintegration, the time was 60 min, TiO_2 0.8 g/l, UV source was UVA lamp, and the pH was changed between 2 and 9. DD changes due to pH change are given in Fig. 6.

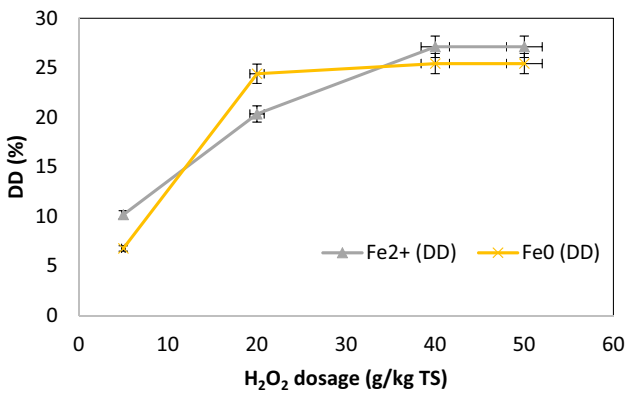

Fig. 4 DD changes depending on H_2O_2 dose (5–50 g/kg TS)

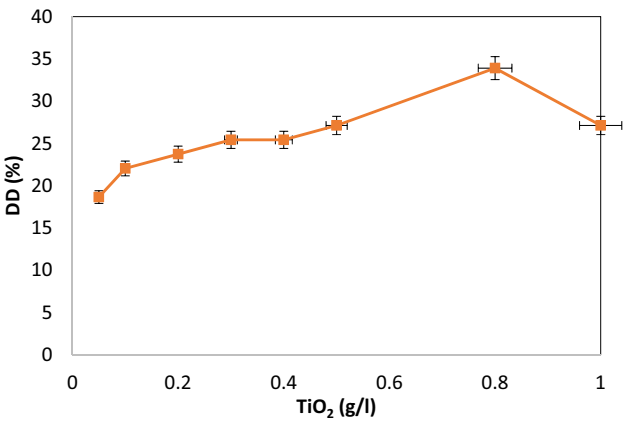

Fig. 5 DD changes depending on TiO_2 dose (0.05–1 g/l)

DD values decrease as the pH value increases. At pH 3, DD was determined as 33.90%, while at pH 9, DD was determined as 25.42%. In similar studies, it has been reported that the appropriate value for pH in the fenton process is in the 2–4 range [51, 54, 57, 60]. In this study, the optimum pH was determined as 3.

Effect of TiO_2/Iron Catalyst

In this study, the effects of use of TiO_2/Fe^{2+} and TiO_2/Fe^0 combinations on disintegration with different UV lamps were investigated by using the previously specified optimum conditions. In this context, TiO_2 0.8 g/l, Fe^{2+} 6 g/kg TS, Fe^0 4 g/kg TS, pH 3 and t 60 min were applied. Different UV lamp efficiencies are shown in Fig. 7.

As seen in Fig. 7, the highest efficiency for DD was achieved in the use of UVB lamp in the TiO_2/Fe^{2+} process, while in the TiO_2/Fe^0 process was obtained in the use of UVA lamp. The highest DD for TiO_2/Fe^{2+} were determined as 25.42%, respectively. Whilst for TiO_2/Fe^0 was 23.73%. Under the same conditions, when TiO_2 was used alone (TiO_2/UV) DD was 33.90%, in Fe^{2+} process DD was 27.12%, and in Fe^0 process DD was 25.42%. When used together (TiO_2/Fe^{2+}), DD decreased to 20.34% (in UVA). In this case, It was found that the use of TiO_2 and iron catalyst (Fe^{2+} or Fe^0) together reduces the disintegration of waste sludge.

When Fe or other metals are added to TiO_2, their surficial complexing properties may change [34].

Effect of Using $TiO_2/Fe^{2+}/H_2O_2$ and $TiO_2/Fe^0/H_2O_2$

In the investigation of the effect of using TiO_2, iron catalyst and H_2O_2 together under different UV sources on sludge disintegration, TiO_2 0.8 g/l; Fe^{2+} 6 g/kg TS, H_2O_2 40 g/kg TS; Fe^0 4 g/kg TS, H_2O_2 20 g/kg TS; pH 3 and t 60 min were applied. The results are given in Fig. 8.

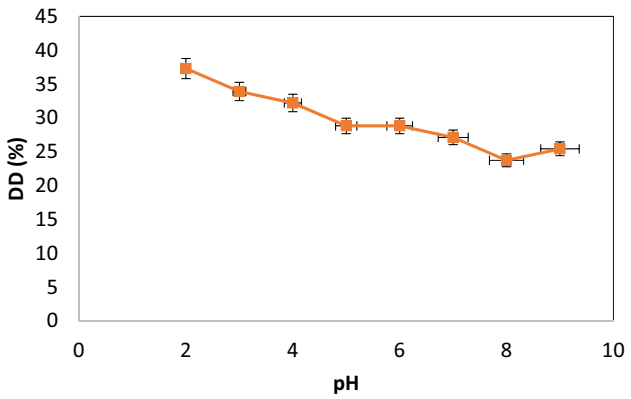

Fig. 6 DD changes depending on pH 2–9

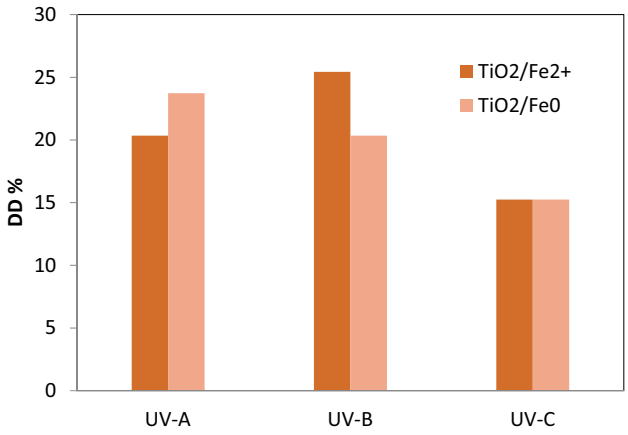

Fig. 7 The effect of TiO_2/iron on DD with different UV Lamps (A/B/C)

As seen in Fig. 8, the highest efficiency in both processes was achieved by using UVB lamps. The highest DD for $TiO_2/Fe^{2+}/H_2O_2$ was determined as 61.02% while for $TiO_2/Fe^0/H_2O2$ was 69.49%. The H_2O_2 added to the iron catalyst with TiO_2 has increased the efficiency considerably. Considering the DD degrees obtained in treatment sludge disintegration, it turns out that the use of these processes is very efficient in sludge disintegration. In addition, UV light flux is one of the important parameters affecting process efficiency in AOP such as Photo-Fenton and Photocatalytic. In literature, it has been reported that light flux affects the removal efficiency in studies with photoreactors with different light fluxes [66, 67].

Kinetic Study

Zero- (Eq. 9), first- (Eq. 10), and second-order (Eq. 11) models were applied to the change data of SCOD concentrations

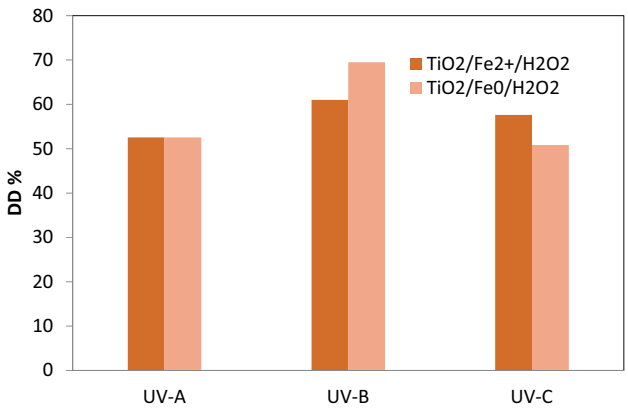

Fig. 8 The effect of $TiO_2/Fe^{2+}/H_2O_2$ and $TiO_2/Fe^0/H_2O_2$ on DD in different UV Lamps (A/B/C)

Table 1 Kinetic constants

UV	Zero-order model		First-order model		Second-order model	
	k_0 (mg/L.min)	R^2	k_1 (1/min)	R^2	k_2 (L/mg.min)	R^2
UVA	6.0798	0.89	0.0416	0.86	0.0003	0.69
UVB	5.7089	0.90	0.0426	0.90	0.0003	0.79
UVC	5.3564	0.93	0.0416	0.86	0.0003	0.80

Table 2 Toxicity analysis results

	Raw sludge	TiO_2/UV	TiO_2/Fe^{2+}/UV	TiO_2/Fe^0/UV	$TiO_2/Fe^{2+}/H_2O_2$/UV	$TiO_2/Fe^0/H_2O_2$/UV
Toxicity GP %	70	70	90	80	80	100

depending on time in optimum conditions for UVA, UVB and UVC. The kinetic parameters calculated for each reaction kinetics are given in Table 1.

$$C = C_0 - k_0.t \tag{9}$$

$$\ln C = \ln C_0 - k_1.t \tag{10}$$

$$\frac{1}{C} = \frac{1}{C_o} + k_2 t \tag{11}$$

In these equations, C_0 initial SCOD concentration (mg/L); C SCOD concentration at any time (mg/L); k_0, k_1 and k_2 are kinetic constants of reaction kinetics of zero-, first-, and second-order models respectively; and t reaction time (minutes).

As can be seen in Table 1, it was determined that all three lamp applications comply with zero-order and first- order kinetics as a function of the SCOD concentration. Besides, R^2 values were similar for both zero degree and 1st degree kinetics. R^2 values varied between 0.89 and 0.93 in the zero-order model, and 0.86–0.90 in the first-order model. When UV-A, UV-B and UV-C were used the value of k_0 constant was calculated as 6.0798, 5.7089 and 5.3564, respectively.

Toxicity

The application of the toxicity test has steadily increased in recent years and has been a useful tool in environmental risk assessment [68]. In this study, toxicity analyzes of raw sludge and disintegrated sludge were performed (Table 2).

As shown in Table 2, for raw mud, the germination percentage was 70%, which means that sprout germination was inhibited. This may be due to harmful organic compound or microorganism in the sludge [69]. After the $TiO_2/Fe^{2+}/H_2O_2$/UV process, the germination percentage increased up to 100%. This proves that toxicity deteriorates significantly after disintegration of the sludge. The reason for this increase is that stubborn or complex organic/inorganic compounds become less toxic [44]. Photocatalytic treatment can disrupt the high organic load in the sludge, ultimately reducing the toxicity of this sludge [70].

Table 3 Changes in the particle size of sludge

	Volume weighted average D (4.3)	d (0.1)	d (0.5)	d (0.9)
Raw sludge	130	18.3	66.3	198
TiO_2/UV	86.5	17.4	57.2	152
TiO_2/Fe^{2+}/UV	85.0	19.5	62.7	159
TiO_2/Fe^0/UV	95.5	18.7	61.4	164
$TiO_2/Fe^{2+}/H_2O_2$/UV	105	17.4	59.3	172
$TiO_2/Fe^0/H_2O_2$/UV	99.6	17.1	58.8	162

Sludge Characterization

Particle Size Distribution Particle Size Distribution was determined at Sivas Cumhuriyet University Advanced Technology Research and Application Center (CÜTAM). In order to observe the effect of disintegration, a particle size analysis was performed under optimum conditions for WAS. Analysis results are given in Table 3. d (0.1), d (0.5), and d (0.9) demonstrate 10, 50, and 90% of particles (in volume) having a diameter lower or equal to d (0.1), d (0.5), and d (0.9), respectively.

During the disintegration, a significant decrease occurs in the particle size in sludge due to the forces applied to the sludge. The disruption of the flock structure in sludge is the main reason for this change. The decrease in the particle size generally provides easier hydrolysis of solids in the sludge due to the increased surface area related with the decrease in the particle volüme [71]. In this study, the particle size decreased in all processes (Table 3). As a result of disintegration (according to volume-weighted average D [4.3]) the volume of sludge decreased by 19.2% to 34.6%. Considering the sludge amounts coming out and disposal expenses of the

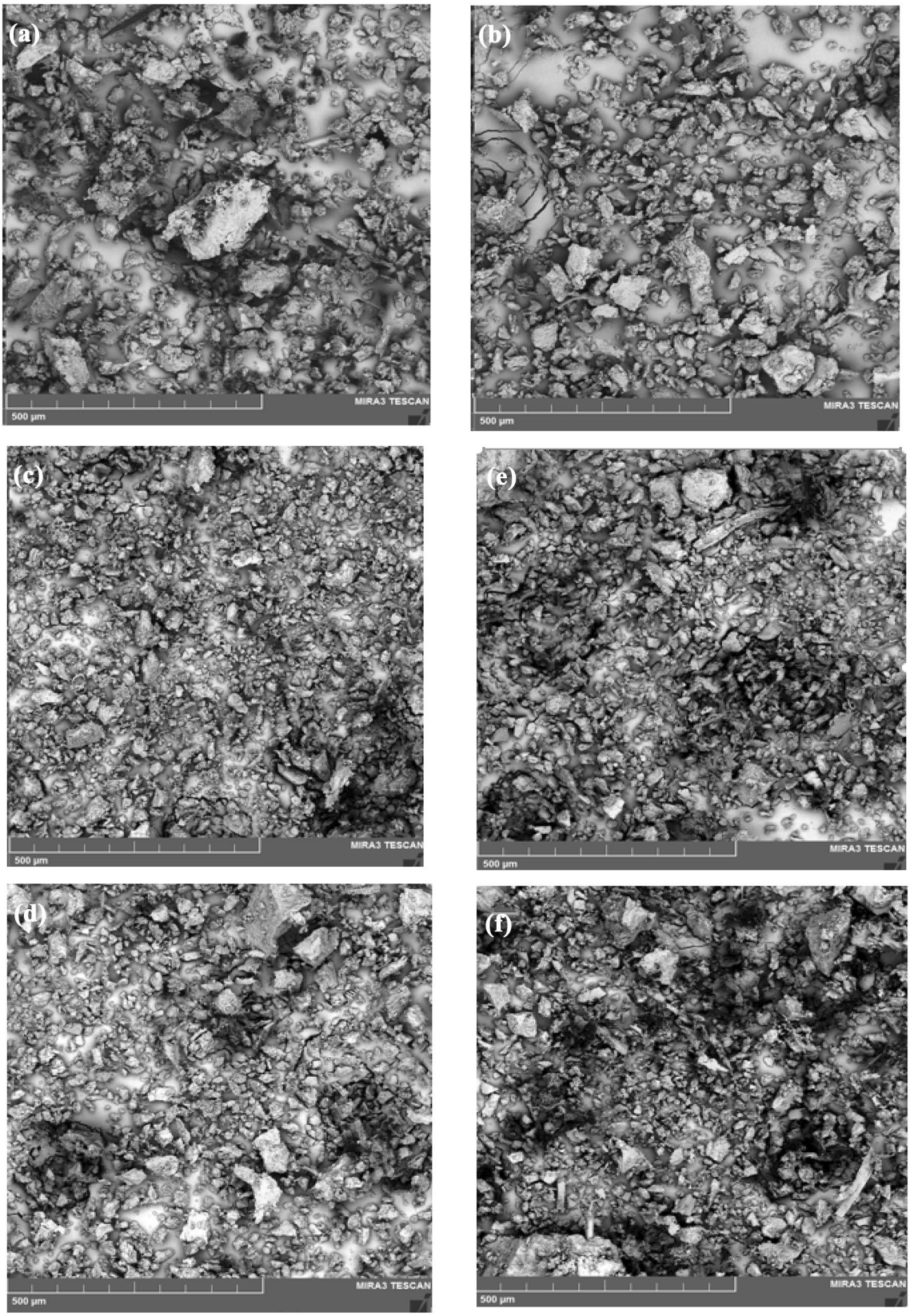

Fig. 9 SEM images; **a** Before disintegration **b** After TiO_2/UV **c** After TiO_2/Fe^{2+}/UV **d** After TiO_2/Fe^0/UV **e** After $TiO_2/Fe^{2+}/H_2O_2$/UV **f** After $TiO_2/Fe^0/H_2O_2$/UV

treatment plants, these reduction rates provide an important advantage.

SEM Analysis SEM analysis was used to analyze the morphology of sludge particles before and after disintegration (Fig. 9). Breaking flocs and microbial cells to remove intracellular liquid is the main purpose of the disintegration process [72]. In this study, it is seen in Fig. 9 that the sludge particle size before and after disintegration has decreased significantly. While the raw sludge particle size (d: 0.9) was 198 µm, the particle size after disintegration varied between 152 and 172 µm (Table 3).

The particle appearance of raw sludge was relatively smooth and larger in size (Fig. 9a). An increase in fragmentation was observed with all processes in consistent with DD. It was also observed that the shape of the particles is irregular and not homogeneous. These particles appear in layered forms. In accordance with the study of Castro et al. [73], large particles with flat edges and sharp corners were observed. The sludge disintegrated by photo fenton shows the highest degree of cell disintegration which confirms a large increase in the DD [74].

Conclusion

Within the scope of the study, photocatalytic disintegration of waste sludge has been investigated under various experimental conditions. In this context, parameters affecting the disintegration degree for different processes have been examined with different UV light fluxes. In addition, kinetic study has been carried out under optimum conditions. The efficiency of TiO_2 used as a catalyst has been investigated in different UV lamps. Besides, the best disintegration process has been tried to be determined with different processes of iron and H_2O_2 added to TiO_2. In this context, TiO_2/UV, TiO_2/Fe^{2+}/UV, TiO_2/Fe^0/UV, $TiO_2/Fe^{2+}/H_2O_2$/UV, $TiO_2/Fe^0/H_2O_2$/UV processes have been applied. In TiO_2/UV application, DD for UVA, UVB and UVC has been 33.9%, 30.51% and 28.81%, respectively. Disintegration efficiency decreases when TiO_2 and iron catalyst are used together. When iron (especially Fe^0) and TiO_2 were used together, DD has decreased significantly. Otherwise, when H_2O_2 was added to this process, it has been found that DD increased dramatically. The highest DD for $TiO_2/Fe^{2+}/H_2O_2$ was determined as 61.02% while for $TiO_2/Fe^0/H_2O2$ was 69.49%. In photocatalytic disintegration process, it has been demonstrated that high levels of disintegration were achieved with H_2O_2 added to the TiO_2 catalyst. Future work should focus on the determination of the influences of photo-Fenton processes on the methaneproduction. Also, comprehensive economical analysis should be investigated.

References

1. Liu, Y.: Chemically reduced excess sludge production in the activated sludge process. Chemosphere **50**(1), 1–7 (2003)
2. Nagao, N., Matsuyama, T., Yamamoto, H., Toda, T.: A novel hybrid system of solid state and submerged fermentation with recycle for organic solid waste treatment. Process Biochem. **39**(1), 37–43 (2003)
3. Øegaard, H.: Sludge minimization technologies-an overview. Water Sci. Technol. **49**(10), 31–40 (2004)
4. Ye, F., Ji, H., Ye, Y.: Effect of potassium ferrate on disintegration of waste activated sludge (WAS). J. Hazard. Mater. **219**, 164–168 (2012)
5. Wang, F., Wang, Y., Ji, M.: Mechanisms and kinetics models for ultrasonic waste activated sludge disintegration. J. Hazard. Mater. **123**(1–3), 145–150 (2005)
6. Yildiz, S., Cömert, A.: Fenton process effect on sludge disintegration. Int. J. Environ. Health Res. **30**(1), 89–104 (2020)
7. Yildiz, S., Oran, E.: Sewage sludge disintegration by electrocoagulation. Int. J. Environ. Health Res. **29**(5), 531–543 (2019)
8. Antoniadis, A., Poulios, I., Nikolakaki, E., Mantzavinos, D.: Sonochemical disinfection of municipal wastewater. J. Hazard. Mater. **146**(3), 492–495 (2007)
9. Machnicka, A., Grubel, K., Suschka, J.: The use of hydrodynamic disintegration as a means to improve anaerobic digestion of activated sludge. WSA (2009). https://doi.org/10.4314/wsa.v35i1.76715
10. Nowicka, E., Machnicka, A., Grübel, K.: Improving of anaerobic digestion by dry ice disintegration of activated sludge. Ecol. Chem. Eng. A **21**(2), 211–219 (2014)
11. Yu, S., Zhang, G., Li, J., Zhao, Z., Kang, X.: Effect of endogenous hydrolytic enzymes pretreatment on the anaerobic digestion of sludge. Biores. Technol. **146**, 758–761 (2013)
12. Liu, Y., Wang, H., Xu, Y., Fang, Y., Chen, X.: Sludge disintegration using a hydrocyclone to improve biological nutrient removal and reduce excess sludge. Sep. Purif. Technol. **177**, 192–199 (2017)
13. Zhao, H., Zhang, P., Zhang, G., Cheng, R.: Enhancement of ultrasonic disintegration of sewage sludge by aeration. J. Environ. Sci. **42**, 163–167 (2016)
14. Wacławek, S., Grübel, K., Chłąd, Z., Dudziak, M., Černík, M.: The impact of oxone on disintegration and dewaterability of waste activated sludge. Water Environ. Res. **88**(2), 152–157 (2016)
15. Kudlek, E.: Identification of degradation by-products of selected pesticides during oxidation and chlorination processes. Ecol. Chem. Eng. S **26**(3), 571–581 (2019)
16. Benitez, F.J., Acero, J.L., Gonzalez, T., Garcia, J.: Organic matter removal from wastewaters of the black olive industry by chemical and biological procedures. Process Biochem. **37**(3), 257–265 (2001)
17. Deng, Y., Englehardt, J.D.: Treatment of landfill leachate by the fenton process. Water Res. **40**(20), 3683–3694 (2006)
18. Ensing, B., Buda, F., Baerends, E.J.: Fenton-like chemistry in water: oxidation catalysis by Fe (III) and H_2O_2. J. Phys. Chem. A **107**(30), 5722–5731 (2003)
19. Wacławek, S., Padil, V.V., Černík, M.: Major advances and challenges in heterogeneous catalysis for environmental applications: a review. Ecol. Chem. Eng. S **25**(1), 9–34 (2018)
20. Qamar, M., Saquib, M., Muneer, M.: Photocatalytic degradation of two selected dye derivatives, chromotrope 2B and amido black 10B, in aqueous suspensions of titanium dioxide. Dyes Pigm. **65**(1), 1–9 (2005)
21. Akpan, U.G., Hameed, B.H.: Parameters affecting the photocatalytic degradation of dyes using TiO_2-based photocatalysts: a review. J. Hazard. Mater. **170**(2–3), 520–529 (2009)

22. Rauf, M., Ashraf, S.S.: Fundamental principles and application of heterogeneous photocatalytic degradation of dyes in solution. Chem. Eng. J. **151**(1–3), 10–18 (2009)
23. Ikeda, K., Sakai, H., Baba, R., Hashimoto, K., Fujishima, A.: Photocatalytic reactions involving radical chain reactions using microelectrodes. J. Phys. Chem. B **101**(14), 2617–2620 (1997)
24. Sakai, H., Baba, R., Hashimoto, K., Fujishima, A., Heller, A.: Local Detection of photoelectrochemically produced H_2O_2 with a "Wired" horseradish peroxidase microsensor. J. Phys. Chem. **99**(31), 11896–11900 (1995). https://doi.org/10.1021/j100031a017
25. Wang, R., Hashimoto, K., Fujishima, A., Chikuni, M., Kojima, E., Kitamura, A., Shimohigoshi, M., Watanabe, T.: Light-induced amphiphilic surfaces. Nature **388**(6641), 431–432 (1997)
26. Deng, Y., Zhao, R.: Advanced oxidation processes (AOPs) in wastewater treatment. Curr. Pollution Rep. **1**(3), 167–176 (2015)
27. Agustina, T.E., Teguh, D., Wijaya, Y., Mermaliandi, F., Bustomi, A., Manalaoon, J., Theodora, J., Rebecca, T.: Study of synthetic dye removal using Fenton/TiO_2, Fenton/UV, and Fenton/TiO_2/UV methods and the application to Jumputan fabric wastewater. Acta Polytech. **59**(6), 527–535 (2019)
28. Sun, Y., Pignatello, J.J.: Photochemical reactions involved in the total mineralization of 2,4-D by iron(3+)/hydrogen peroxide/UV. Environ. Sci. Technol. **27**(2), 304–310 (1993)
29. Rajeshwar, K.: Photochemical strategies for abating environmental pollution. Chem. Ind. **12**, 454–458 (1996)
30. Yu, G., Zhu, W., Yang, Z., Li, Z.: Semiconductor photocatalytic oxidation of H-acid aqueous solution. Chemosphere **36**(12), 2673–2681 (1998)
31. Noorjahan, M., Reddy, M.P., Kumari, V.D., Lavedrine, B., Boule, P., Subrahmanyam, M.: Photocatalytic degradation of H-acid over a novel TiO_2 thin film fixed bed reactor and in aqueous suspensions. J. Photochem. Photobiol. A **156**(1–3), 179–187 (2003)
32. Mohanty, S., Rao, N.N., Khare, P., Kaul, S.N.: A coupled photocatalytic–biological process for degradation of 1-amino-8-naphthol-3, 6-disulfonic acid (H-acid). Water Res. **39**(20), 5064–5070 (2005)
33. Sauer, T.P., Casaril, L., Oberziner, A.L.B., José, H.J., Moreira, R.D.: Advanced oxidation processes applied to tannery wastewater containing direct black 38-elimination and degradation kinetics. J. Hazard. Mater. **135**(1), 274–279 (2006)
34. Arana, J., Melián, J.H., Rodrıguez, J.D., Dıaz, O.G., Viera, A., Pena, J.P., Sosa, P.M.M., Jiménez, V.E.: TiO_2-photocatalysis as a tertiary treatment of naturally treated wastewater. Catal. Today **76**(2–4), 279–289 (2002)
35. Muruganandham, M., Selvam, K., Swaminathan, M.: A comparative study of quantum yield and electrical energy per order (EEo) for advanced oxidative decolourisation of reactive azo dyes by UV light. J. Hazard. Mater. **144**(1), 316–322 (2007)
36. Catalkaya, E.C., Kargi, F.: Advanced oxidation treatment of pulp mill effluent for TOC and toxicity removals. J. Environ. Manage. **87**(3), 396–404 (2008)
37. Garcia, J.C., Oliveira, J.L., Silva, A.E.C., Oliveira, C.C., Nozaki, J., de Souza, N.E.: Comparative study of the degradation of real textile effluents by photocatalytic reactions involving UV/TiO_2/H_2O_2 and UV/Fe^{2+}/H_2O_2 systems. J. Hazard. Mater. **147**(1), 105–110 (2007)
38. Camacho, P., Déléris, S., Geaugey, V., Ginestet, P., Paul, E.: A comparative study between mechanical, thermal and oxidative disintegration techniques of waste activated sludge. Water Sci. Technol. **46**(10), 79–87 (2002)
39. Rocher, M., Roux, G., Goma, G., Pilas Begue, A., Louvel, L., Rols, J.: Excess sludge reduction in activated sludge processes by integrating biomass alkaline heat treatment. Water Sci. Technol. **44**(2–3), 437–444 (2001)
40. Kallel, M., Belaid, C., Mechichi, T., Ksibi, M., Elleuch, B.: Removal of organic load and phenolic compounds from olive mill wastewater by fenton oxidation with zero-valent iron. Chem. Eng. J. **150**(2), 391–395 (2009)
41. Eaton, A., Clesceri, L.S., Rice, E.W., Greenberg, A.E., Franson, M.: APHA: Standard methods for the examination of water and wastewater, Centennial APHA, Washington, DC (2005)
42. Huan, L., Yiying, J., Mahar, R.B., Zhiyu, W., Yongfeng, N.: Effects of ultrasonic disintegration on sludge microbial activity and dewaterability. J. Hazard. Mater. **161**(2), 1421–1426 (2009)
43. Sarat Chandra, T., Malik, S.N., Suvidha, G., Padmere, M.L., Shanmugam, P., Mudliar, S.N.: Wet air oxidation pretreatment of biomethanated distillery effluent: mapping pretreatment efficiency in terms color, toxicity reduction and biogas generation. Biores. Technol. **158**, 135–140 (2014)
44. Malik, S.N., Ghosh, P.C., Vaidya, A.N., Waindeskar, V., Das, S., Mudliar, S.N.: Comparison of coagulation, ozone and ferrate treatment processes for color, COD and toxicity removal from complex textile wastewater. Water Sci. Technol. **76**(5), 1001–1010 (2017)
45. Parsons, S.: Advanced oxidation processes for water and wastewater treatment. IWA publishing, London UK (2004)
46. Egemen, E., Corpening, J., Nirmalakhandan, N.: Evaluation of an ozonation system for reduced waste sludge generation. Water Sci. Technol. **44**(2–3), 445–452 (2001)
47. Park, K.Y., Lee, J.W., Ahn, K.H., Maeng, S.K., Hwang, J.H., Song, K.G.: Ozone disintegration of excess biomass and application to nitrogen removal. Water Environ. Res. **76**(2), 162–167 (2004)
48. Déléris, S., Paul, E., Audic, J.M., Roustan, M., Debellefontaine, H.: Effect of ozonation on activated sludge solubilization and mineralization. Ozone Sci. Eng. **22**(5), 473–486 (2000)
49. Vlyssides, A., Karlis, P.: Thermal-alkaline solubilization of waste activated sludge as a pre-treatment stage for anaerobic digestion. Biores. Technol. **91**(2), 201–206 (2004)
50. Malato, S., Fernández-Ibáñez, P., Maldonado, M.I., Blanco, J., Gernjak, W.: Decontamination and disinfection of water by solar photocatalysis: recent overview and trends. Catal. Today **147**(1), 1–59 (2009)
51. Matavos-Aramyan, S., Moussavi, M.: Advances in fenton and fenton based oxidation processes for industrial effluent contaminants control-a review. Int. J. Environ. Sci. Nat. Resour. **2**(4), 1–18 (2017)
52. Nikravan, A.: Amoxicillin and ampicillin removal from wastewater by fenton and photo-fenton processes. Institute of Science and Technology, Hacettepe Unv (2015)
53. Ebrahiem, E.E., Al-Maghrabi, M.N., Mobarki, A.R.: Removal of organic pollutants from industrial wastewater by applying photo-fenton oxidation technology. Arab. J. Chem. **10**, 1674–1679 (2017)
54. GilPavas, E., Dobrosz-Gómez, I., Gómez-García, M.Á.: Coagulation-flocculation sequential with fenton or photo-fenton processes as an alternative for the industrial textile wastewater treatment. J. Environ. Manage. **191**, 189–197 (2017)
55. Nadeem, K., Guyer, G.T., Dizge, N.: Polishing of biologically treated textile wastewater through AOPs and recycling for wet processing. J. Water Process Eng. **20**, 29–39 (2017)
56. Ishak, S., Malakahmad, A.: Optimization of fenton process for refinery wastewater biodegradability augmentation. Korean J. Chem. Eng. **30**(5), 1083–1090 (2013)
57. Abedinzadeh, N., Shariat, M., Monavari, S.M., Pendashteh, A.: Evaluation of color and COD removal by fenton from biologically (SBR) pre-treated pulp and paper wastewater. Process Saf. Environ. Prot. **116**, 82–91 (2018)

58. Saini, R., Kumar, P.: Optimization of chlorpyrifos degradation by fenton oxidation using CCD and ANFIS computing technique. J. Environ. Chem. Eng. **4**(3), 2952–2963 (2016)
59. Kim, J.R., Kan, E.: Heterogeneous photo-fenton oxidation of methylene blue using CdS-carbon nanotube/TiO_2 under visible light. J. Ind. Eng. Chem. **21**, 644–652 (2015)
60. Pouran, S.R., Aziz, A.A., Daud, W.M.A.W.: Review on the main advances in photo-fenton oxidation system for recalcitrant wastewaters. J. Ind. Eng. Chem. **21**, 53–69 (2015)
61. Santos-Juanes, L., Einschlag, F.G., Amat, A.M., Arques, A.: Combining ZVI reduction with photo-fenton process for the removal of persistent pollutants. Chem. Eng. J. **310**, 484–490 (2017)
62. Giannakis, S., Liu, S., Carratalà, A., Rtimi, S., Talebi Amiri, M., Bensimon, M., Pulgarin, C.: Iron oxide-mediated semiconductor photocatalysis vs. heterogeneous photo-fenton treatment of viruses in wastewater. Impact of the oxide particle size. J. Hazard. Mater. **339**, 223–231 (2017)
63. Papoutsakis, S., Pulgarin, C., Oller, I., Sánchez-Moreno, R., Malato, S.: Enhancement of the fenton and photo-fenton processes by components found in wastewater from the industrial processing of natural products: the possibilities of cork boiling wastewater reuse. Chem. Eng. J. **304**, 890–896 (2016)
64. Jańczyk, A., Krakowska, E., Stochel, G., Macyk, W.: Singlet oxygen photogeneration at surface modified titanium dioxide. J. Am. Chem. Soc. **128**(49), 15574–15575 (2006)
65. Kang, J.W., Hung, H.M., Lin, A., Hoffmann, M.R.: Sonolytic destruction of methyl tert-butyl ether by ultrasonic irradiation: the role of O_3, H_2O_2, frequency, and power density. Environ. Sci. Technol. **33**(18), 3199–3205 (1999)
66. Qiao, R.P., Li, N., Qi, X.H., Wang, Q.S., Zhuang, Y.Y.: Degradation of microcystin-RR by UV radiation in the presence of hydrogen peroxide. Toxicon **45**(6), 745–752 (2005)
67. Xu, B., Gao, N.Y., Cheng, H., Xia, S.J., Rui, M., Zhao, D.D.: Oxidative degradation of dimethyl phthalate (DMP) by UV/H_2O_2 process. J. Hazard. Mater. **162**(2), 954–959 (2009)
68. Ioannou, L., Fatta-Kassinos, D.: Solar photo-Fenton oxidation against the bioresistant fractions of winery wastewater. J. Environ. Chem. Eng. **1**(4), 703–712 (2013)
69. Flores, N., Sharif, F., Yasri, N., Brillas, E., Sirés, I., Roberts, E.P.: Removal of tyrosol from water by adsorption on carbonaceous materials and electrochemical advanced oxidation processes. Chemosphere **201**, 807–815 (2018)
70. Welter, J.B., Soares, E.V., Rotta, E.H., Seibert, D.: Bioassays and Zahn-Wellens test assessment on landfill leachate treated by photo-fenton process. J. Environ. Chem. Eng. **6**(1), 1390–1395 (2018)
71. Müller, J.A., Winter, A., Struenkmann, G.: Investigation and assessment of sludge pre-treatment processes. Water Sci. Technol. **49**(10), 97–104 (2004)
72. Bohdziewicz, J., Kuglarz, M., Grűbel, K.: Influence of microwave pre-treatment on the digestion and higienisation of waste activated sludge/Wpływ Dezintegracji Mikrofalowej Na proces Fermentacji Oraz Higienizacji Nadmiernych Osadów Ściekowych. Ecol. Chem. Eng. S **21**(3), 447–464 (2014)
73. Castro, C.A., Centeno, A., Giraldo, S.A.: Iron promotion of the TiO_2 photosensitization process towards the photocatalytic oxidation of azo dyes under solar-simulated light irradiation. Mater. Chem. Phys. **129**(3), 1176–1183 (2011)
74. Braguglia, C.M., Gianico, A., Mininni, G.: Effect of ultrasound on particle surface charge and filterability during sludge anaerobic digestion. Water Sci Technol. **60**, 2025–2033 (2009)